Table 2. Rotational constants (B) for specific vibrational levels of CH_3^+.

ν_2	ν_4	B (cm^{-1}) theory*	B (cm^{-1}) experiment
0	0	9.42	9.3623†
1	0	9.11	9.1
2	0	8.53	8.6
3	0	8.26	8.5
0	1	9.57	9.1
1	1	9.27	9.1

*(24). †(23).

frequencies are compared with previous experimental results and theoretical values in Table 1, and rotational constants for each vibrational level are presented in Table 2 and compared to theoretical results (*21*). Previous experimental values for vibrational frequencies have been reported only for the ν_2 (umbrella) (*22*) and ν_3 (C–H asymmetric stretch) modes (*23*, *24*), and there is considerable uncertainty in the former (see Table 1). A tentative assignment of ν_1 was made in our earlier low-resolution study, but it is apparent now that this was probably a single rotational line for $\nu_2 = 3$. Aside from Oka's value for the vibrationless level and the strongly allowed ν_3 fundamental, there have been no experimentally determined rotational constants for this system; we thus compare the rotational constants in Table 2 to theoretical calculations (*25*).

These results also provide insight into the dissociation dynamics of the process. The observed distribution principally shows evidence for a progression in umbrella-mode excitation, which may be readily understood by considering the change in the CH_3 geometry from the near-tetrahedral configuration of the parent molecule to the stiffly planar CH_3^+. In addition to the umbrella-mode progression, we also see evidence for some ν_4 excitation, both alone and in combination with one quanta of ν_2. Although not necessarily anticipated by a naïve view of the dynamics, it may be that coupling of the initially prepared Rydberg state to the ion pair state is favored by this in-plane bend excitation.

References and Notes

1. J. Berkowitz, *Photoabsorption, Photoionization and Photoelectron Spectroscopy* (Academic Press, New York, 1979).
2. E. Hirota, *Chem. Rev.* **92**, 141 (1992).
3. ———, *Annu. Rev. Prog. Chem. C* **96**, 95 (2000).
4. J. D. D. Martin, J. W. Hepburn, *Phys. Rev. Lett.* **79**, 3154 (1997).
5. ———, *J. Chem. Phys.* **109**, 8139 (1998).
6. M. Ahmed, D. S. Peterka, P. Regan, X. H. Liu, A. G. Suits, *Chem. Phys. Lett.* **339**, 203 (2001).
7. M. V. Frohne, thesis, Kansas State University, Manhattan, KS (1994).
8. A. Eppink, D. H. Parker, *Rev. Sci. Instrum.* **68**, 3477 (1997).
9. M. Kawasaki, K. Suto, Y. Sato, Y. Matsumi, R. Bersohn, *J. Phys. Chem.* **100**, 19853 (1996).
10. Y. Hikosaka, J. H. D. Eland, *Rapid Commun. Mass Spectrom.* **14**, 2305 (2000).
11. M. Ahmed, D. Blunt, D. Chen, A. G. Suits, *J. Chem. Phys.* **106**, 7617 (1997).
12. A low field ionization stage injects the ions into high field acceleration and focusing lenses, resulting in reduced aberration as compared to single-stage velocity mapping (X. Liu, R. L. Gross, A. G. Suits, unpublished results).
13. B. Y. Chang, R. C. Hoetzlein, J. A. Mueller, J. D. Geiser, P. L. Houston, *Rev. Sci. Instrum.* **69**, 1665 (1998).
14. W. M. Jackson, D. Xu, R. J. Price, K. L. McNesby, I. A. McLaren, in *Imaging in Chemical Dynamics*, A. G. Suits, R. E. Continetti, Eds. (American Chemical Society, Washington, DC, 2000), pp. 103–25.
15. M. J. J. Vrakking, *Rev. Sci. Instrum.* **72**, 4084 (2001).
16. L. V. Gurvich, I. V. Veyts, C. B. Alcock, *Thermodynamics Properties of Individual Substances* (Hemisphere, New York, 1989).
17. J. A. Blush, P. Chen, R. T. Wiedmann, M. G. White, *J. Chem. Phys.* **98**, 3557 (1993).
18. M. Litorja, B. Ruscic, *J. Chem. Phys.* **107**, 9852 (1997).
19. M. Zahedi, J. A. Harrison, J. W. Nibler, *J. Chem. Phys.* **100**, 4043 (1994).
20. The vibrational modes for CH_3^+ are ν_1, C-H symmetric stretch; ν_2, out-of-the-plane bend; ν_3, degenerate C-H stretch; ν_4, degenerate bend.
21. For the ortho forms, the nuclear spin factor g_{NK} = 0 and 4 for J odd and even, respectively, of vibrational levels with even quanta of ν_2 excitation. For odd quanta of ν_2 excitation, the situation is reversed, and only odd rotational levels are permitted. For the para modifications, this constraint is not present, and J odd or even may be equally populated.
22. R. V. Olkhov, S. A. Nizkorodov, O. Dopfer, *J. Chem. Phys.* **108**, 10046 (1998).
23. J. Dyke, N. Jonathan, E. Lee, A. Morris, *J. Chem. Soc. Faraday Trans. 2* **72**, 1385 (1976).
24. M. W. Crofton, W. A. Kreiner, M. F. Jagod, B. D. Rehfuss, T. Oka, *J. Chem. Phys.* **83**, 3702 (1985).
25. M. W. Crofton, M. F. Jagod, B. D. Rehfuss, W. A. Kreiner, T. Oka, *J. Chem. Phys.* **88**, 666 (1988).
26. W. P. Kraemer, V. Spirko, *J. Mol. Spec.* **149**, 235 (1991).

27. We thank G. Hall and T. Sears for valuable discussions. Supported by the Director, Office of Energy Research, Office of Basic Energy Sciences, Chemical Sciences Division, of the U.S. Department of Energy under contract DE-AC02-98CH1086.

26 September 2001; accepted 8 November 2001

Regional $^{14}CO_2$ Offsets in the Troposphere: Magnitude, Mechanisms, and Consequences

Bernd Kromer,[1]* Sturt W. Manning,[3] Peter Ian Kuniholm,[4] Maryanne W. Newton,[4] Marco Spurk,[5] Ingeborg Levin[2]

Radiocarbon dating methods typically assume that there are no significant tropospheric $^{14}CO_2$ gradients within the low- to mid-latitude zone of the Northern Hemisphere. Comparison of tree ring ^{14}C data from southern Germany and Anatolia supports this assumption in general but also documents episodes of significant short-term regional $^{14}CO_2$ offsets. We suggest that the offset is caused by an enhanced seasonal $^{14}CO_2$ cycle, with seasonally peaked flux of stratospheric ^{14}C into the troposphere during periods of low solar magnetic activity, coinciding with substantial atmospheric cooling. Short-term episodes of regional $^{14}CO_2$ offsets are important to palaeoclimate studies and to high-resolution archaeological dating.

The basic assumption about the atmospheric distribution of ^{14}C is that, although sources of ^{14}C-depleted C (such as outgassing of CO_2 from the ocean mixed layer) or ^{14}C-enriched C (such as intrusion of newly produced ^{14}C from the stratosphere) are restricted to certain areas and thus could leave a regional $^{14}CO_2$ imprint, rapid atmospheric mixing produces an efficient dispersion of $^{14}CO_2$ gradients. Hence, over even short time spans, on the order of 1 month, there are approximately uniform hemispheric levels of ^{14}C. In consequence, a cornerstone of ^{14}C dating is the assumption of a spatially uniform $^{14}CO_2$ source level during carbon uptake by plants, allowing us to provide and employ a single universal ^{14}C data set for the calibration of the ^{14}C time scale (*1*, *2*).

Support for the assumption that any regional $^{14}CO_2$ differences are small and may be ignored (that is, they are close to the detection limits of

[1]Heidelberger Akademie der Wissenschaften, [2]Institut für Umweltphysik der Universität Heidelberg, Im Neuenheimer Feld 229, D-69120 Heidelberg, Germany. [3]Department of Archaeology, University of Reading, Post Office Box 218 Whiteknights, Reading RG6 6AA, UK. [4]The Malcolm and Carolyn Wiener Laboratory for Aegean and Near Eastern Dendrochronology, B-48 Goldwin Smith Hall, Cornell University, Ithaca, NY 14853–3201, USA. [5]Institut für Botanik-210, Universität Hohenheim, D-70593 Stuttgart, Germany.

*To whom correspondence should be addressed. E-mail: bernd.kromer@iup.uni-heidelberg.de

the current radiocarbon technique) comes from carbon cycle modeling. Braziunas *et al.* (*3*) used a coupled atmosphere-ocean general circulation model (GCM) to calculate the preindustrial global atmospheric $^{14}CO_2$ distribution. For the low- and mid-latitudes of either hemisphere, they found zonal mean meridional ^{14}C activity gradients of only about 1 per mil (‰), which is equivalent to a difference of 8 ^{14}C years in measurement determination. In view of achievable measurement precision of no better than 2 to 3‰ even at high-precision ^{14}C laboratories, this work shows that the low- to mid-latitudes of each hemisphere are uniform in $^{14}CO_2$ concentration for practical purposes. Only at high latitudes does the $^{14}CO_2$ gradient increase to up to 6‰ (equivalent to an apparent ^{14}C age difference of 48 years) (*2*–*4*).

The ability to directly detect $^{14}CO_2$ gradients depends on measurement precision. The most extensive work has been carried out during the construction of the high-precision ^{14}C calibration data sets, when absolutely dated tree ring chronologies from various mid-latitude regions of Europe and North America were compared to study the magnitude of regional ^{14}C offsets at several, up to millennia-long, time intervals of the Holocene. The results of such studies have been inconsistent about whether measurable ^{14}C gradients exist (*5*–*8*).

The majority of the data document mid-latitude mean regional differences well below 10 ^{14}C years (albeit only if the corrections of the Belfast laboratory are to be applied), but several shorter intervals show regional differences between zero and up to several decades. The latter are significant if correct. Some workers have suggested that changes in oceanic and atmospheric circulation patterns may be responsible for such offsets (*2*, *6*).

It is important to resolve this disagreement, because, if substantial regional offsets in ^{14}C levels are real within the core low- to mid-latitude zone of the Northern Hemisphere, the calibration of ^{14}C ages into calendar years would require regional corrections, in the same way as is done for marine ^{14}C ages (ΔR values). This issue is particularly relevant for building an accurate time frame for the prehistory of the eastern Mediterranean, because there small but highly important discrepancies between radiocarbon dates and dates derived from the interpretation of historical and protohistorical evidence have led to several decades of controversy, such as the debate concerning the age of the Thera volcano eruption (*9*).

We therefore designed a three-stage study [the Eastern Mediterranean Radiocarbon Intercomparison Project (EMRCP)] to establish the extent, if any, of a regional ^{14}C gradient between a key region and a tree species used to build the international standard high-precision calibration curve (*1*, *10*) [German oak (GeO) from southern Germany] and the eastern Mediterranean region, using wood from Anatolia. ^{14}C measurements were performed at the Heidelberg Radiocarbon Laboratory. First, we determined the overall dating precision of the Heidelberg laboratory by replicating the ^{14}C calibration data set, based on GeO, in the 17th and 16th centuries B.C. Second, we determined the ^{14}C ages of decades of wood that grew at exactly the same time from absolutely dated wood samples from Anatolia and southern Germany grown in the 15th to 17th centuries A.D. Third, using the information gained in the first two stages, we then explored the anchoring of a floating Anatolian tree ring chronology in the 2nd millennium B.C. to the ^{14}C data sets from the absolutely dated GeO and Irish oak (IrO) chronologies.

For the first stage of EMRCP, we selected 22 decades of GeO in the interval 1490–1710 B.C., from the middle Main river, southern Germany. This section had been previously measured in the Seattle ^{14}C laboratory (*11*). For stage 2 of EMRCP, we selected decadal samples from two absolutely dated tree ring chronologies: Turkish pine (TuP) (*Pinus nigra*) from Çatacık in western Anatolia and GeO (*Quercus robur*) from historical buildings in southern Germany. These sequences cover the interval 1420–1649 A.D.; that is, a span of 23 decades (*12*).

An independent assessment of laboratory errors is possible through our replication of the GeO data comprising part of the INTCAL98 calibration data set (*13*). In Fig. 1, our measurements are compared to those of the Seattle ^{14}C laboratory. The mean difference between the Heidelberg-Seattle decadal data is 2.3 ^{14}C years. The observed versus expected standard deviation of the differences is 29.0 versus 22.5 ^{14}C years. The increase in variance is dominated by the decade with midpoint at 1675 B.C., with an observed difference of 80 ^{14}C years (3.8σ variation based on quoted measurement errors). When this decade is omitted, the observed versus expected standard deviation drops to 23.8 versus 22.5 ^{14}C years. We repeated the Heidelberg measurements of the decades with midpoints at 1655–1675 B.C. (note the additional GeO data in Fig. 1), with results identical to the previous ones. The bidecadal ^{14}C age of IrO (*1*, *7*) at 1670 B.C. is 3344 ± 21 ^{14}C years, which does not help to resolve the discrepancy satisfactorily. Therefore, we decided to omit the decade with midpoint at 1675 B.C. from the comparison. The total increase in the variance of the pairs is explained by an additional, unknown error of 7.8 ^{14}C years (18.3 ^{14}C years if the decade with midpoint at 1675 BC is included), caused by either one of the two laboratories or by both of them. From this comparison, we conclude that a conservative upper limit of an additional, unknown laboratory error for the Heidelberg facility is 8 ^{14}C years, included in all data presented here.

A comparison of ^{14}C ages of pairs of same-age decades from GeO and TuP wood samples is shown in Fig. 2. The mean absolute difference of the 23 pairs of GeO-TuP is 1.4 ^{14}C years, indicating a regional offset between Central Europe and Anatolia that is negligible. However, a clear trend is visible in the data, with all TuP ages being older than GeO in the interval A.D. 1440–1540 (mean difference between TuP and GeO, 17 ^{14}C years) but mostly younger in the intervals before and after, A.D. 1420–1440 and A.D. 1550–1640 (mean difference between TuP and GeO, –14 ^{14}C years for A.D. 1550–1640). The TuP > GeO episode occurs at a time of strongly rising atmospheric ^{14}C levels, which leads to the rapid decrease of ^{14}C ages as compared to calendar ages; this episode also corresponds with the Spörer minimum of solar activity (A.D. 1416–1534) (*14*) and the associated cooler climate episode in the mid-15th century A.D. in the Northern Hemisphere that has been detected in many studies (*15*, *16*).

We observe the same pattern when we try to anchor the floating Aegean Bronze Age juniper chronology (ABJ) (*17*) to our GeO data (Fig. 1)

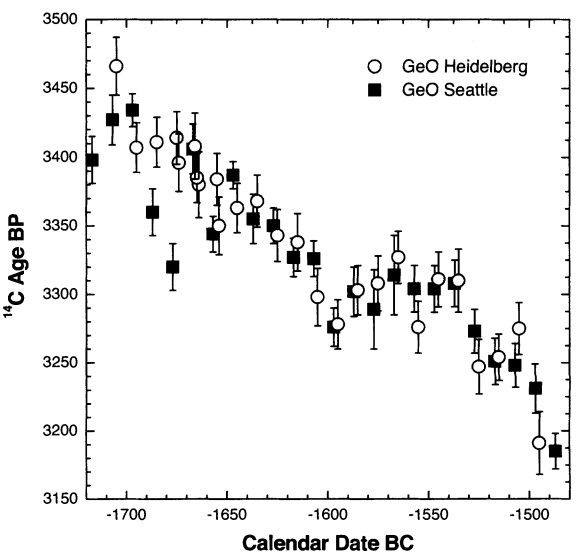

Fig. 1. Comparison of Heidelberg and Seattle (*13*) measurements on similarly sourced GeO decadal samples.

and the ^{14}C calibration curve (*1*). Using 52 ABJ decadal ^{14}C age determinations made on samples of *Juniperus foetidissima* and *J. excelsa*, we can obtain a match (*18*) only when we accept that the ABJ ^{14}C data in the early 8th century B.C. are offset by ~30 ^{14}C years with respect to the ^{14}C data based on Central European wood (Fig. 3 and inset). Again, we note that the ^{14}C levels differ significantly, and for a short period consistently, only for intervals of strongly changing atmospheric ^{14}C, coincident with widespread cooling in the Northern Hemisphere (*19*, *20*).

What could cause such a difference in the atmospheric ^{14}C level between the two regions? The key to the answer may lie in the magnitude, timing, and location of injection of stratospheric ^{14}C into the troposphere, combined with the mechanisms of carbon storage in tree rings. Based on the mean lifetime of ^{14}C of 8267 years, in a steady state, every year 1/8‰ of the total ^{14}C inventory is replenished by ^{14}C production in the stratosphere and troposphere. Ultimately, ^{14}C reaches the deep ocean, which contains most of the global ^{14}C inventory; but mixing within the stratosphere, latitude-dependent cross-tropopause exchange, carbon and ^{14}C exchange across the sea surface, and deep ocean ventilation—all of which operate on a wide range of time scales—attenuate and cause a phase shift of the ^{14}C source. Because the atmosphere holds just ~1.5% of the global ^{14}C inventory, it is a sensitive monitor of transient changes in any of the transport stages. In fact, from our present-day tropospheric ^{14}C monitoring network (*4*) and from modeling bomb radiocarbon (*21*), we deduce a preindustrial/prebomb seasonal ^{14}C component of ~4‰ activity variation between low winter/spring and maximum summer activity. Thus, depending on the rate of carbon uptake during the growing season and the phase relation of the growing season between two regions, the comparison of annual tree rings may show part of this seasonal cycle: an earlier onset of warmth, followed by restricted water availability, largely constrain average tree growth in the Mediterranean to spring and early summer, whereas Central European oaks lay down a substantial contribution of the overall carbon storage in their annual rings later, in July and August.

For most of the time covered by our comparison, the net effect is too small to be detected at the level of measurement precision. However, the amplitude of the seasonal cycle is proportional to the ^{14}C influx from the stratosphere. During times of "deep" solar minima (*22*), the ^{14}C production (*23*) and hence ^{14}C flux were doubled as compared to the average of the 11-year solar cycle [figure 8. of (*24*)] at high latitudes. Thus, the seasonal cycle becomes notable, and we can explain the difference in magnitude of the regional ^{14}C gradient between the A.D. and the B.C. event because the ^{14}C increase in the 8th century B.C. was 50% higher than in the Spörer minimum episode.

The recording of the seasonal ^{14}C signal by tree rings also may have been amplified by climate change. The two events are part of widespread hemispheric cooling episodes (*15*, *19*, *20*): the initial phases of the Little Ice Age after the Medieval Warm Period, and the wet and cold earlier 8th century B.C. For this type of event, a cyclonic circulation and higher frequency of cold polar air in the North Atlantic and northwestern Europe is assumed, with the eastern Mediterranean in antiphase (*25*). Thus, while Central European trees may have had their growing season shifted to later in the summer, because of the cold (continental-type) winters, the vegetation in the Mediterranean may have enjoyed favorable moisture and temperature conditions leading to early growth (*26*). Furthermore, during deep solar activity minima, the solar ultraviolet flux was considerably reduced (*27*), leading to changes in stratospheric heating and circulation (*28*–*30*). Thus, the partitioning of major mechanisms in stratosphere-troposphere ^{14}C exchange, as well as tropospheric wave propagation, may have been notably different during these intervals, adding to the ^{14}C seasonality.

Thus, although the general calibration of ^{14}C ages is only marginally affected by our findings, and the standard calibration curves may be used with confidence in most cases, at certain times significant deviations occur. For example, the revised best estimate dates for the

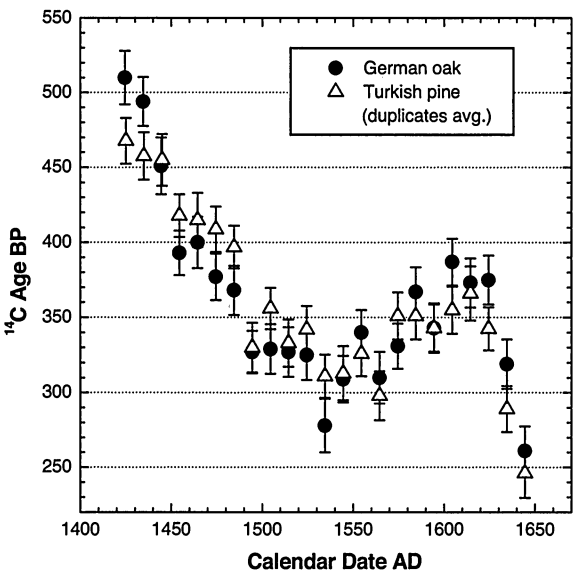

Fig. 2. ^{14}C ages of decadal samples of GeO and TuP, grown contemporaneously.

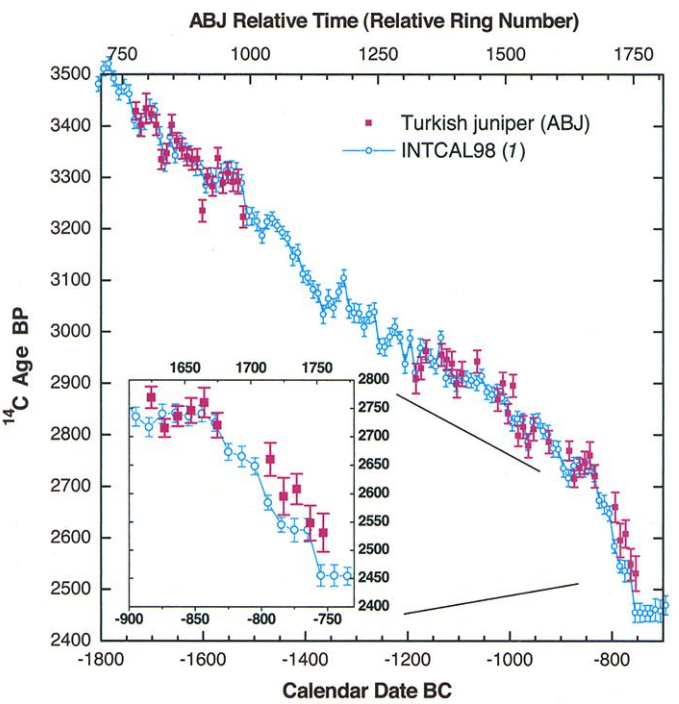

Fig. 3. Wiggle-match of 52 ^{14}C decadal age determinations of the floating Aegean Bronze Age juniper chronology to the internationally recommended INTCAL98 calibration data set (*1*): See (*31*) for details and discussion. In the interval from the mid-9th to mid-8th centuries B.C. (inset), a period of rising atmospheric ^{14}C levels (strongly declining ^{14}C ages), a significant ^{14}C age difference exists between Central Europe and Anatolia.

floating Bronze-Iron Age Aegean dendrochronology (*31*) now must be shifted to ages ~22 years older—a matter of no little importance for archaeologists (*9*). Finally, it is clear that high-precision ^{14}C analyses provide a valuable tool for studying decadal- to century-scale atmospheric dynamics in the past.

References and Notes

1. M. Stuiver *et al.*, *Radiocarbon* **40**, 1041 (1998).
2. M. Stuiver, T. F. Braziunas, *Geophys. Res. Lett.* **25**, 329 (1998).
3. T. F. Braziunas, I. Y. Fung, M. Stuiver, *Global Biogeochem. Cycles* **9**, 565 (1995).
4. I. Levin, V. Hesshaimer, *Radiocarbon* **42**, 69 (2000).
5. M. Stuiver, G. W. Pearson, *Radiocarbon* **35**, 1 (1993).
6. F. G. McCormac, M. G. L. Baillie, J. R. Pilcher, *Radiocarbon* **37**, 395 (1995).
7. G. W. Pearson, M. Stuiver, *Radiocarbon* **35**, 25 (1993).
8. J. C. Vogel, A. Fuls, E. Visser, B. Becker, *Radiocarbon* **35**, 73 (1993).
9. S. W. Manning, *A Test of Time: The Volcano of Thera and the Chronology and History of the Aegean and East Mediterranean in the Mid Second Millennium BC* (Oxbow Books, Oxford, 1999).
10. M. Spurk *et al.*, *Radiocarbon* **40**, 1 (1998).
11. M. Stuiver, B. Becker, *Radiocarbon* **35**, 35 (1993).
12. Samples (19 to 25 g) were pretreated with the AAA sequence (*32*, *33*). All samples were combusted to CO_2, and their ^{14}C activity was determined by CO_2 gas counting for a total counting time of 7 to 10 days. The error as reported consists of Poisson counting statistics (~1.1 ‰) and regression analyses of background versus barometric pressure and standard versus gas purity (*34*). We consider our approach to the error calculation to be conservative, as the regression analysis includes empirical evidence of otherwise unspecified fluctuations in counter-performance in addition to the purely Poisson error components. The total error (1σ) of the ^{14}C age determination of a decadal wood sample was between 10 and 19 years for full-sized samples. For some replicates, we had less wood available (8 g), increasing the error to up to 29 years for these samples.
13. M. Stuiver, P. J. Reimer, T. F. Braziunas, *Radiocarbon* **40**, 1127 (1998).
14. M. Stuiver, P. Quay, *Science* **207**, 11 (1980).
15. H. H. Lamb, *Climate, History and the Modern World* (Routledge, London, 1995).
16. K. R. Briffa *et al.*, *J. Geophys. Res.* **106**, 2929 (2001). These authors use a novel approach to temperature reconstruction, which offers warmer summer temperatures for Siberia for the 15th century A.D. in their final temperature reconstruction, at odds, as the authors note (on p. 2938), with other methods of temperature estimation (see their figure 4) and with most other Northern Hemisphere reconstructions (see their plate 3), which find a clear cool period from around 1450 A.D.
17. P. I. Kuniholm *et al.*, *Nature* **381**, 780 (1996).
18. C. B. Ramsey, *Radiocarbon* **37**, 425 (1995).
19. B. van Geel *et al.*, *Radiocarbon* **40**, 531 (1998).
20. G. Bond *et al.*, *Science* 15 November 2001 (10.1126/science. 1065680).
21. V. Hesshaimer, thesis, Univ. of Heidelberg, Heidelberg, Germany (1997).
22. E. Nesme-Ribes, D. Sokoloff, J. C. Ribes, M. Kremliovsky, *NATO ASI Ser.* **I**, 71 (1994).
23. E. Bard, G. Raisbeck, F. Yiou, J. Jouzel, *Tellus* **52B**, 985 (2000).
24. J. Masarik, J. Beer, *J. Geophys. Res.* **104**, 12099 (1999).
25. J. Hurrell, *Science* **269**, 676 (1995).
26. F. M. Chmielewski, T. Rotzer, *Agric. Forest Meteorol.* **108**, 101 (2001).
27. J. Lean, D. Rind, *J. Clim.* **11**, 3069 (1998).
28. N. K. Balachandran, D. Rind, *J. Clim.* **8**, 2059 (1995).
29. D. T. Shindell, G. A. Schmidt, R. L. Miller, D. Rind, *J. Geophys. Res.* **106**, 7193 (2001).
30. H. van Loon, K. Labitzke, *J. Clim.* **11**, 1529 (1998).
31. S. W. Manning, B. Kromer, P. I. Kuniholm, M. W. Newton, *Science* **294**, 2532 (2001).
32. B. Kromer, B. Becker, *Radiocarbon* **35**, 125 (1993).
33. The TuP samples were, in addition, pretreated in a Soxhlet extraction to remove resins. We did not further convert the samples to cellulose, because in numerous studies we determined that the results from our version of the AAA sequence do not differ from those of the full cellulose pretreatment [see, for example, table 2 of (*1*)].
34. B. Kromer, K.-O. Münnich, in *Radiocarbon After Four Decades*, R. E. Taylor, A. Long, R. S. Kra, Eds. (Springer, New York, 1992), pp. 184–197.

35. We thank P. Reimer, M. Stuiver, C. Bronk Ramsey, M. Bell, D. Wagenbach, P. Valdes, and J. Chiment for discussions; M. J. Bruce and K. B. Harris for manuscript preparation; and two anonymous *Science* reviewers. We thank the Institute for Aegean Prehistory for funding the majority of this work; we also acknowledge the support of NSF, the Malcolm H. Wiener Foundation, and the Federal Ministry of Education and Research (Bundesministerium für Bildung und Forschung).

10 September 2001; accepted 27 November 2001
Published online 6 December 2001;
10.1126/science.1066114
Include this information when citing this paper.

Anatolian Tree Rings and a New Chronology for the East Mediterranean Bronze-Iron Ages

Sturt W. Manning,[1]* Bernd Kromer,[2] Peter Ian Kuniholm,[3] Maryanne W. Newton[3]

We report an extensive program of high-precision radiocarbon dating to establish the best date for a floating 1599-year Anatolian tree ring chronology that spans the later third millennium B.C. through the earlier first millennium B.C. This chronology is directly associated with a number of key sites and ancient personages. A previously suggested dating is withdrawn and is replaced by a robust new date fix 22 (+4 or −7) years earlier. These new radiocarbon wiggle-matched dates offer a unique independent resource for establishing the precise chronology of the ancient Near East and Aegean and help resolve, among others, a long-standing debate in favor of the so-called Middle Mesopotamian chronology.

Over a period of 30 years, the Aegean Dendrochronology Project has built a robust, long, but floating tree ring chronology with the use of timbers collected from major archaeological monuments in Anatolia dating from the later third millennium B.C. through the earlier first millennium B.C. This chronology is central to the dating of some 22 Bronze and Iron Age sites (*1*) and forms a pivotal reference point for the archaeology and history of the eastern Mediterranean. The core of the chronology consists of 1026 years of cross-dated and well-replicated tree rings preserved at the Phrygian capital city of Gordion, particularly from the Midas Mound Tumulus grave chamber, the world's oldest standing wooden building (*2*, *3*). We report

[1]Department of Archaeology, University of Reading, Post Office Box 218 Whiteknights, Reading RG6 6AA, UK. [2]Heidelberger Akademie der Wissenschaften, Im Neuenheimer Feld 229, D-69120 Heidelberg, Germany. [3]The Malcolm and Carolyn Wiener Laboratory for Aegean and Near Eastern Dendrochronology, B-48 Goldwin Smith Hall, Cornell University, Ithaca, NY 14853–3201, USA.

*To whom correspondence should be addressed. E-mail: S.W.Manning@reading.ac.uk

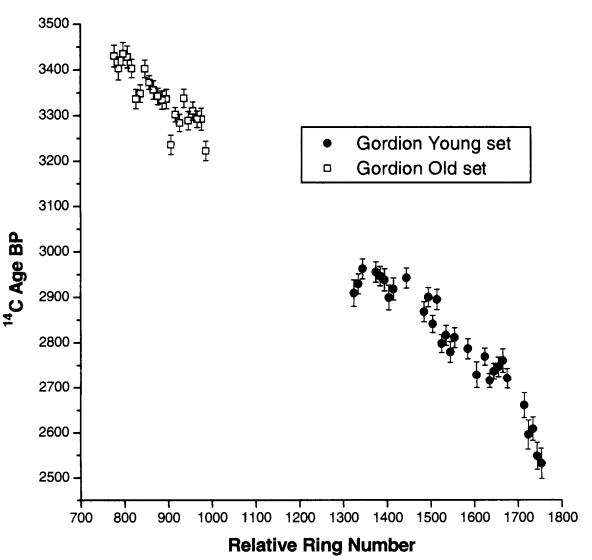

Fig. 1. Radiocarbon data with 1σ errors from decadal tree ring samples from wood series recovered from structures at Gordion, central Anatolia. The Old set comprises decades centered on relative rings 777–987. The Young set comprises decades centered on relative rings 1325–1754. Radiocarbon measurements were carried out at Heidelberg according to standard procedures (*42*, *43*). Data shown here and used in this study include a small additional error factor determined from a detailed intercomparison of measurements by the Heidelberg and Seattle laboratories on mid–second millennium B.C. south German oak of known age (*12*); total stated errors are thus regarded as conservative.